

Article

Network-Level Hierarchical Bottleneck Congestion Control Method for a Mixed Traffic Network

Yuncheng Zeng^{1,2}, Minhua Shao^{1,2,*}  and Lijun Sun^{1,2}

¹ College of Transportation Engineering, Tongji University, 4800 Cao'an Highway, Shanghai 201804, China; zengyuncheng@tongji.edu.com (Y.Z.); ljsun@tongji.edu.cn (L.S.)

² Key Laboratory of Road and Traffic Engineering of the Ministry of Education, Tongji University, Shanghai 201804, China

* Correspondence: minhuashao@163.com; Tel.: +86-135-6409-9112

Abstract: Due to the escalating transportation demand and the significant ramifications of traffic congestion, there is an imperative to investigate the sources of congestion, known as “congestion bottlenecks”. The implementation of control methods ahead of the occurrence of congestion is crucial. Connected and autonomous vehicles (CAVs) have a high potential within the field of traffic control. CAVs are exceptionally controllable and facilitate management feasibility. This study utilizes the high compliance of CAVs to provide an effective solution for the congestion management problem at the network level when mixed traffic flows are saturated. A linear programming model to reduce average travel time over the road network is developed. By utilizing a genetic algorithm, the optimal traffic demand regulation scheme can be obtained and the departure time of CAVs optimized. The effectiveness of the proposed method is validated through simulation across various road network scales, CAVs penetration rates, and controlled CAV proportions. The proposed method can only control a specific amount of CAVs, which, according to an analysis of the simulation results, significantly improves the performance of the transportation system. The importance of employing advanced control methods to improve the sustainability of urban transportation development and the travel experience is underscored in the conclusion.

Keywords: sustainable transport development; congestion control; mixed traffic system; connected and autonomous vehicles; traffic demand



Citation: Zeng, Y.; Shao, M.; Sun, L. Network-Level Hierarchical Bottleneck Congestion Control Method for a Mixed Traffic Network. *Sustainability* **2023**, *15*, 16160. <https://doi.org/10.3390/su152316160>

Received: 21 September 2023
Revised: 16 November 2023
Accepted: 19 November 2023
Published: 21 November 2023



Copyright: © 2023 by the authors. Licensee MDPI, Basel, Switzerland. This article is an open access article distributed under the terms and conditions of the Creative Commons Attribution (CC BY) license (<https://creativecommons.org/licenses/by/4.0/>).

1. Introduction

1.1. Background

Nowadays, numerous cities worldwide struggle with significant challenges due to traffic congestion. All of the ten cities that ranked highest in terms of hours lost per driver due to traffic congestion in 2022 suffered at least 105 lost hours. This amount is equivalent to wasting more than four full days stuck behind the wheel [1]. Apart from the loss of time, the economic losses resulting from traffic congestion are also very significant [2–5]. In 2022, the financial burden imposed on drivers due to traffic congestion in the United States amounted to more than 81 billion dollars. Similarly, the United Kingdom had a cost of 9.5 billion pounds, while Germany incurred a cost of 3.9 billion euros [2]. Meanwhile, in the context of urban environments, transportation stands out as a major contributor to air pollution [6–9]. In the year 2019, the transportation sector in the United States was responsible for the emission of around 190 million tons of carbon dioxide (CO₂), constituting almost 28% of the overall domestic emissions [6]. In addition to CO₂, which contributes to the greenhouse effect, vehicle exhaust emissions may discharge carbon monoxide, nitrogen oxides, and volatile organic compounds, all of which can exert an even more detrimental influence on air quality. Additionally, traffic congestion threatens the safety of travelers. According to the National Highway Traffic Safety Administration (NHTSA), the year 2018 had more than 35,000 traffic crash fatalities. It is noticeable that a considerable proportion of these

incidents can be attributed either directly or indirectly to congestion [10]. These presented data emphasize the severe consequences associated with traffic congestion. The problems that come with increasing traffic congestion are threatening sustainable mobility for our future [11].

The current state of traffic congestion is already of great concern; however, cities are experiencing continued growth and the demand for transportation is expected to substantially increase over the next few years [10]. Consequently, this will result in frequent and extensive congestion within the transportation system. The escalating traffic demand and the severe ramifications of traffic congestion have an imperative to investigate the sources of congestion, known as “congestion bottlenecks”, and to develop methods for managing traffic conditions at these bottlenecks. Bottlenecks can cause rapid oscillations in vehicle speeds and densities, which can rapidly propagate upstream [12]. The concept of a bottleneck was first proposed by Vickrey [13]. Bottlenecks are described localized obstructions to traffic flow by Federal Highway Administration (FHWA) in 2011 [14]. Bottlenecks are deficiencies in traffic operations caused by traffic inflows that exceed the design capacity, resulting in abnormal traffic flow conditions. The extended consequences of bottlenecks have devastating consequences not just in the localized areas where the bottlenecks occur, but over a far wider stretch, exposing more travelers in danger [10].

Managing traffic congestion effectively has been a difficult challenge for transportation organizations. Urban traffic control (UTC) systems have also been continuously updated and innovated to keep up with the increasing traffic demands [11,15,16]. Since UTC systems usually rely on drivers’ high levels of compliance, the management’s effectiveness depends on the drivers’ awareness and willingness, hence limiting the control strategy’s possible application. Fortunately, among the various new techniques developed for traffic control, connected and automated vehicles (CAVs) are believed to have great potential [17]. Generally, vehicles that are capable of communicating with other vehicles (vehicle-to-vehicle or V2V), infrastructure (vehicle-to-infrastructure or V2I), and other traffic participants including pedestrians and cyclists (V2X) are denoted as connected vehicles (CVs) [18,19]. Fully automated vehicles (AVs) are those in which “the vehicle can do all the driving in all circumstances. The human occupants are just passengers and need never be involved in driving” [20]. Thus, a CAV should be a vehicle that can perform the operational of a traditional vehicle on its own and can communicate with nearby vehicles and infrastructure for safer driving [21].

With rapid advances in wireless communication, sensing, and computing technologies, it is anticipated that CAVs will soon extend beyond experimental environments and be extensively deployed alongside traditional human-driven vehicles (HDVs) on roadways. In contrast to HDVs and AVs, CAVs make full use of real-time road information to plan routes by control terminals, and a high degree of compliance ensures effective traffic management. Even though a lot of progress has been made so far, it will still take a relatively long time for CAVs to achieve complete automation and have a high market penetration. It is expected that in the near future, we will observe both HDVs and CAVs on the roads [22]. Managing and controlling mixed traffic system holds both significant promise and challenges.

In such a situation where traffic congestion can have significant consequences, transportation demand keeps growing, and technologies related to CAVs are fast developing. The primary goal of this research is to use advanced CAVs to alleviate traffic congestion at bottlenecks.

1.2. Literature Review

Alleviating traffic congestion at bottlenecks can bring network-wide improvement [23]. Improving traffic conditions at bottlenecks is frequently the most effective strategy to enhance traffic flow and relieve congestion. Numerous researchers have studied both the nature and prediction of flow breakdown as well as mitigation strategies to alleviate or prevent congestion [10]. Several methods have been proposed to mitigate traffic flow breakdown, including regulating arrival traffic demand and making the capacity larger.

The improvement of traffic capacity can only be achieved by the implementation of vehicle control measures that aim to decrease headway and increase speeds. These measures are particularly relevant when the possibility of reconstructing the road through engineering interventions is not being taken into consideration. The most significant method of vehicle control that can accomplish this has been thought to be AVs or CAVs. Nonetheless, the academic research on controlling AVs or CAVs remains scant and in its infancy [24]. Moreover, at the current stage of AVs development, the free flow speed, minimum headway, and maximum acceleration and deceleration values of AVs fail to align with the prevailing optimistic predictions in most of the literature, which suggest that these characteristics can be steadily distributed at better values. According to calculations based on AVS trajectories measured in recent open road areas, the actual free flow speed and dispersion of AVs are much slower than those of HDVs. The minimum headway is also greater than that of HDVs, and the maximum acceleration and deceleration values are similar to those of HDVs, but more volatile [25].

For these reasons, our research will concentrate on road-based traffic control systems capable of regulating traffic flow. Road-based traffic control systems are utilized to regulate the traffic flow by implementing various strategies. These strategies include limiting the inflow of traffic into the network through ramp management, regulating the existing traffic within the network through mainstream control or speed harmonization, and routing traffic flows on alternative paths within the network through route guidance [10,24].

1.2.1. Ramp Management

Numerous academics have developed control methods to efficiently merge CAVs from multi-lane ramps. Luo et al. [26] proposed control strategies to allow vehicles from different lanes to pass through conflict points, with the goal of minimizing delay and fuel consumption. Furthermore, for the problem of merging vehicles in different lanes, a multi-lane centralized cooperative control strategy based on a cooperative game was designed by Yang et al. [27]. The cooperative game approach is employed to determine the optimal merging order of vehicles in different lanes, considering driving efficiency, comfort and fuel consumption as cost functions in the merging control area. In the mixed traffic environment where CAVs and HDVs coexist, Liu et al. [28] introduced a two-level hierarchical cooperative on-ramp merging control strategy for CAVs. The objective of this strategy is to optimize the trajectories of CAVs while ensuring safety, allowing them to merge onto the main road in a flexible manner. To confirm the effectiveness of the proposed methods, the recommended control strategies have been simulated in each of the aforementioned literatures.

1.2.2. Speed Harmonization

Speed harmonization (SH) aims to reduce the speed variance of the vehicles within an area of interest [10,17,29–34]. The SPECIALIST model [35] is an innovative example of SH that employs the concepts from Kinematic Waves [36,37] to limit the inflow to the shockwaves by decreasing the speed limit. The efficacy of the technique was evaluated on a Dutch roadway, and the results indicated that it could improve throughput by effectively resolving moving shockwaves [38]. Chen and Ahn [39] devised a speed coordination system based on shockwave theory to address the issue of the bottleneck. In a simulated analysis, their technique was able to increase throughput at fixed bottlenecks, while concurrently mitigating shockwave intensity, resulting in smoother speed transitions. Elfar [34] presented a predictive speed coordination system that can figure out where traffic congestion will happen and broadcasts updated speed limitations to CAVs to relieve it. The system does this with the help of machine learning algorithms and detailed vehicle trajectories broadcast by CAVs. Ha et al. [10] present a control model based on reinforcement learning for multi-intelligent CAVs that can operate in mixed traffic (CAVs and HDVs). The results show that CAVs can significantly alleviate bottlenecks in freeway traffic, even when CAVs account for only 10% of corridor traffic.

The suitability of speed harmonization may not be appropriate for road network with high saturation where vehicle speeds vary widely. In such cases, speed harmonization may be difficult to implement.

1.2.3. Route Guidance

Guo et al. [11] conducted a comprehensive analysis of the existing literature and observed a limit of research related to road network-wide traffic control systems based on CVs. Research on traffic control at the network level mainly focuses on path planning and traffic assignment. However, most studies primarily concentrate on static traffic assignment, whereas the dynamic control of CAVs' paths to improve the overall performance of the traffic network under mixed traffic flow is still in its early stages of research. Guo et al. [22] proposed a dynamic bi-level optimal control problem to improve the systemic performance of the traffic network. The upper-level problem involves CAVs' route control, while the lower-level problem deals with HDVs' route selection. They established an optimal control problem with equilibrium constraints' (OCPEC) model. The objective for CAVs is to minimize the total travel time of the system, in accordance with the principles of dynamic system optimal (DSO) [40,41]. On the other hand, HDVs operate in a self-interested manner, aiming to minimize their individual travel costs, and based on the principles of dynamic user equilibrium (DUE) [40,41] within the traffic network.

Traffic assignment methods can effectively improve the overall performance of the traffic system when the system is either uncongested or experiencing only minor congested. However, their effectiveness is limited in highly saturated traffic systems. Furthermore, the practical applicability of these methods for traffic management in real-world traffic systems remains limited due to the required detailed control over a large number of vehicles. The primary obstacle is to attaining optimal control effectiveness while minimizing costs.

1.2.4. Network-Level Hybrid Traffic Control Method

In recent years, there has been an increasing number of studies concentrating on hybrid traffic control method at the network level. Moradi et al. [42] proposed an integrated three-layer hierarchical framework. This framework incorporates intersection controllers located at various intersections within the network, network controllers for regulating the inflow of traffic into the network, and a sequential phase controller for optimizing the intersection signals. The primary objective of this framework is to facilitate orderly, continuous, and efficient traffic movement of vehicles through the traffic road network. In 2023, Guo et al. [43] proposed a general multi-scale modeling and control framework for urban traffic control with CAVs. This framework addresses both the faster-scale vehicle control problem and the slower-scale signal control problem. The work in this paper is the first step towards the establishment of the comprehensive theory, as well as the development of analysis and solution methods for a general multi-scale control framework for UTC.

Based on the limitations of existing research and drawing inspiration from Vickrey's communication travel time control [13] as well as the findings of Moradi and Guo [42,43], this study designs a network-level hierarchical bottleneck congestion control method that takes into account the spatiotemporal propagation characteristics of traffic flow. The majority of the aforementioned publications have employed simulation to confirm the efficacy of the proposed control strategies, the current state of CAVs' development, and the impracticability of testing them in real saturated traffic environments. Thus, this research also investigates the control method through simulation.

The subsequent sections of this manuscript are structured as follows. Section 2 provides an overview of the proposed traffic regulation method for a mixed traffic system on road networks. It includes various tasks such as acquiring traffic data, identifying congestion bottleneck, dividing control layers, as well as developing and solving of the linear programming model. Following that, in Section 3, two road networks, small-scale and large-scale, are constructed to simulate traffic and validate the effectiveness of the

proposed control system. A comprehensive evaluation is conducted on the efficacy of the control approach across various CAVs' penetration rates and CAVs' control proportion. In the final section, Section 4, concluding observations and recommendations for further research are presented.

2. Method

This section presents a traffic regulation approach for mixed traffic systems. Figure 1 shows the basic workflow of the Network-Level Hierarchical Bottleneck Congestion Control Method. To begin with, we have to collect traffic data for further examination and management. With the help of these data, we are able to identify the recurring congestion bottleneck and use it as the primary control point. We then divide the control layers based on the distance that each road edge is to the congestion bottleneck. Our main objective is to regulating the traffic demand within different layers at different time periods. Based on this, we create a linear programming model whose goal is to reduce the average travel time. This model allows us to control the departure time of particular CAVs, consequently decreasing the whole transport system's travel time and delay.

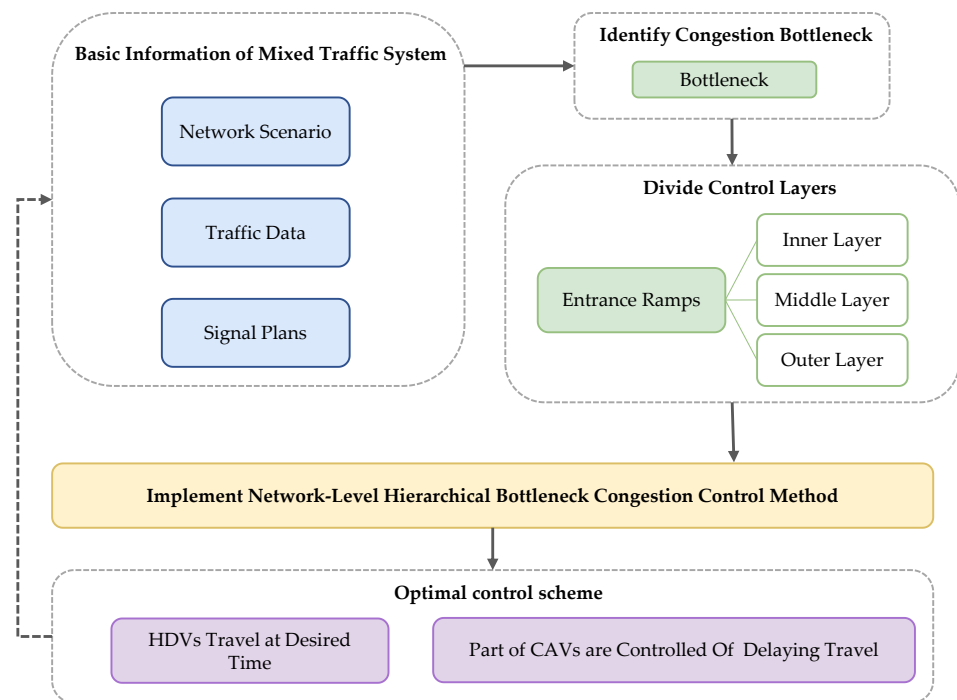


Figure 1. The proposed control method's fundamental procedure.

The following assumptions are made for this search. The traffic system can be classified into two distinct kinds of travelers: CAVs and HDVs. Due to the utilization of sophisticated sensors and wireless communication devices, CAVs possess the capability to engage in real-time communication with both infrastructure and other CAVs.

Thanks to the utilization of advanced sensors and wireless communication devices, CAVs can communicate in real time with both the infrastructure and other CAVs. Additionally, they may receive instructions from traffic managers and obtain pertinent information about the vehicles in their immediate environment. HDVs are totally uncontrollable, while CAVs demonstrate complete controllability and will adhere to traffic management' guidance.

Some of the basic parameters used subsequently are as follows: There are N_{edges} edges in the road network and the edges are denoted by e_j , $j \in \{1, 2, \dots, N_{edges}\}$. The length of edge e_j is denoted by l_{e_j} . The road network has a total of N_{tazs} transportation analysis zones (TAZs), TAZs are denoted by taz_k , $k \in \{1, 2, \dots, N_{tazs}\}$. The number of road edges

included in a TAZ taz_k is denoted by N_{taz_k} . The traffic flow has a total of $N_{vehicles}$ vehicles, vehicle $i \in \{1, 2, \dots, N_{vehicles}\}$.

2.1. Traffic Data Acquisition

A range of techniques are employed to collect fundamental data on the mixed traffic system, such as the utilization of roadside cameras, sensor-equipped CAVs, and loop detection. Traffic signal plans are supplementary to the network topology and traffic flow data (vehicle trajectory or traffic flow data recorded by detectors), which are considered essential. The preprocessing of the data is necessary for real applications, and this can be accomplished by employing the method outlined in our previous research publication [44]. The traffic data in the simulation is gathered from passing vehicles using instantaneous loop detectors. These detectors are strategically positioned in each lane, both upstream and downstream of each edge. This data includes the identification number, time, and instantaneous speed. Table 1 displays the traffic flow data that was utilized in this investigation. With regard to CAVs, comprehensive data can be gathered through detection and communication devices installed on CAVs, as well as the detectors positioned throughout the road network.

Table 1. An illustration of fundamental traffic flow data.

Parameter	Meaning	Example
id	Detector number	"e_121047599_0_1"
time	Moment of data collection	"4.19"
state	Vehicle status (including enter, stay, leave)	"enter"
vehID	Vehicle number captured	"121047599_375822882#1_HDV_time4200.0"
speed	Instantaneous speed of each vehicle (m/s)	"10.14"
length	Length of each vehicle (m)	"5.00"
type	Vehicle type (includes both HDVs and CAVs)	"HDV"

The detectors deployed upstream and downstream of the road edge e_j are denoted by $d_{in}^{e_j}$ and $d_{out}^{e_j}$, respectively. The detector $d_{in}^{e_j}$ detects vehicle i at moment $t_i^{e_j, in}$, and the detector $d_{out}^{e_j}$ detects vehicle i at moment $t_i^{e_j, out}$.

2.2. Congestion Bottleneck Identification

The traditional method for identifying recurrent congestion bottlenecks involves assessing three key factors: congestion intensity, congestion duration, and frequency of recurrent occurrences [45]. It implies that, based on the initial traffic data, it is necessary to first ascertain the spatial average speed of each road edge for every time interval as a preliminary step. The following procedure is used to compute the spatial average speed for each road edge based on the identified traffic data. The travel time t_i^j of vehicle i on road edge e_j is first calculated by using the moment that vehicle i passes upstream and downstream of the edge e_j and is calculated by Equation (1):

$$t_i^j = t_i^{e_j, out} - t_i^{e_j, in}, \quad (1)$$

where variables $t_i^{e_j, in}$ and $t_i^{e_j, out}$ denote the moment detectors $d_{in}^{e_j}$ and $d_{out}^{e_j}$ detect vehicle j .

Then, the spatially average travel time of the road edge e_j over the time period $[t, t + T_{\text{interval}})$ is denoted by $\bar{T}_{[t, t + T_{\text{interval}}]}^{e_j}$ and is calculated by the Equation (2):

$$\bar{T}_{[t, t + T_{\text{interval}}]}^{e_j} = \frac{\sum_{i \in J_{[t, t + T_{\text{interval}}]}^{e_j}} t_i^{e_j}}{|J_{[t, t + T_{\text{interval}}]}^{e_j}|}, \quad (2)$$

where $t_i^{e_j}$ is the travel time of vehicle i on road edge e_j calculated in Equation (1). The variable $J_{[t, t + T_{\text{interval}}]}^{e_j}$ is the set of vehicles detected by detector $d_{\text{in}}^{e_j}$ or $d_{\text{out}}^{e_j}$ during the time period $[t, t + T_{\text{interval}})$. Moreover, the variable $|J_{[t, t + T_{\text{interval}}]}^{e_j}|$ denotes the length of the vehicle set $J_{[t, t + T_{\text{interval}}]}^{e_j}$, i.e., the total number of vehicles passing through the roadway edge e_j during the time period $[t, t + T_{\text{interval}})$. $t \in \{0, T_{\text{interval}}, 2T_{\text{interval}}, \dots, (n-1)T_{\text{interval}}\}$, where T_{interval} indicates the time period interval, and n denotes the number of time periods with time interval T_{interval} included in the total analysis time T_{max} . How T_{max} is determined we will discuss in the subsequent section. n can be calculated by the Equation (3):

$$n = \left\lceil \frac{T_{\text{max}}}{T_{\text{interval}}} \right\rceil \quad (3)$$

Finally, divide the length l_{e_j} by the spatially average travel time $\bar{T}_{[t, t + T_{\text{interval}}]}^{e_j}$ to obtain the spatially averaged vehicle speed $\bar{v}_{[t, t + T_{\text{interval}}]}^{e_j}$ of the road edge e_j during this time period:

$$\bar{v}_{[t, t + T_{\text{interval}}]}^{e_j} = \frac{l_{e_j}}{\bar{T}_{[t, t + T_{\text{interval}}]}^{e_j}} \quad (4)$$

Find the time period when the average speed of each edge $\bar{v}_{[t, t + T_{\text{interval}}]}^{e_j}$ in the road network is lower than the critical speed of $v^* = 12$ (m/s) [44], which is defined as the occurrence of congestion. Additionally, statistically record the initial occurrence of congestion for each edge, as well as the frequency of congestion. The road edge that experiences congestion the earliest is considered to be the congestion bottleneck among those edges that exhibit the highest frequency of congestion. In the context of an extensive road network, there exist multiple bottlenecks.

The traffic situation in the vicinity of this bottleneck and its future state are constantly being monitored. The time T^* when congestion first occurs are predicted as the target moments for control. The aim of the control measures is to proactively prevent or mitigate congestion, in terms of both temporal and spatial aspects. It is crucial to execute these measures beforehand, prior to the actual occurrence of congestion.

2.3. Control Layers Division

It can be shown that traffic demand originated from road edges further away from the congested bottleneck takes longer temporally to propagate to the bottleneck based on the spatial and temporal propagation characteristics of traffic flows. Because of this, these demands need to be regulated earlier.

The road edges other than the bottleneck are separated into three layers according to the network connectivity in order to simplify the calculation process: the inner layer, middle layer, and the outer layer. The inner, middle, and outer layers are radial ranges of 0 to l_0 , l_0 to $2l_0$ and $2l_0$ to $3l_0$ distances from the bottleneck, respectively. The corresponding time periods for the implementation of control measures for each layer is $T^* - t_0$ to T^* , $T^* - 2t_0$ to $T^* - t_0$, and $T^* - 3t_0$ to $T^* - 2t_0$, respectively, before the moment T^* when congestion first occurs at the bottleneck. Therefore, specific time periods for implementing the control measures is determined by $T_{\text{control}} = [T^* - 3t_0, T^*]$. l_0 and t_0 are quantities

related to the scale of the road network. The set of CAVs controlled in each layer at the corresponding time periods are denoted as J_{in}^* , J_{mid}^* , and J_{out}^* , respectively. The set of control CAVs in each layer for the relevant time period is shown in Figure 2.

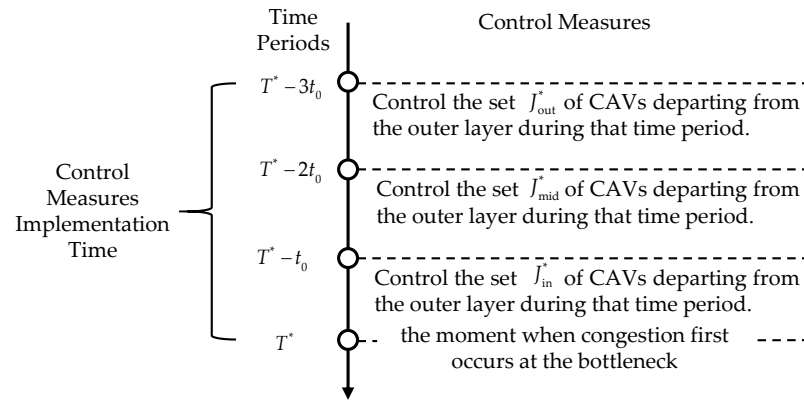


Figure 2. The set of control CAVs in each layer for the relevant time period.

2.4. Control Method Implementation

Prior to the initial occurrence of the traffic congested moment (T^*) at the bottleneck, controls are implemented. In this study, the focus is only on managing the schedule of CAVs enter the network. The following linear programming model is used to determine the exact regulatory scheme.

2.4.1. Objective Function

The objective of this work is to minimize the average travel time of the entire mixed transportation system by developing a mixed integer linear programming formulation. The objective function, denoted by ϕ , is utilized to measure the optimization objective of our model. To be more precise, Equation (5) describes how to minimize the average travel time components: the average departure delay before travelling named \bar{t}_{DD} , the average travel duration in the network named \bar{t}_{TD} , and the average extra departure delay for the controlled CAVs named \bar{t}_{eTD} .

$$\min \phi = \min(\bar{t}_{DD} + \bar{t}_{TD} + \bar{t}_{eTD}) = \min \frac{\sum_{i \in \{1, 2, \dots, N_{\text{vehicles}}\}} (t_{DD}^i + t_{TD}^i) + \sum_{j^* \in \{J_{in}^*, J_{mid}^*, J_{out}^*\}} t_{eTD}^{j^*}}{N_{\text{vehicles}}}, \tag{5}$$

where t_{DD}^i and t_{TD}^i represent the departure delay and travel duration for vehicle i , respectively. $t_{eTD}^{j^*}$ represents the extra departure delay for the controlled CAV j^* , $j \in \{J_{in}^*, J_{mid}^*, J_{out}^*\}$. J_{in}^* , J_{mid}^* , and J_{out}^* is the set of CAVs controlled in each layer, respectively. N_{vehicles} is the total number of vehicles in the traffic flow.

HDVs tend to be arbitrary and unpredictable, as they can enter the traffic network in accordance with the individual preferences of the travelers. The departure delay of HDVs is determined by the density of traffic in the entrance lane or the mainline that connects to the lane from which they enter. The departure delay of a CAV is also affected by the density of traffic in the connecting mainline and entrance lane. In contrast, controlled CAV are restricted to entering the network during designated periods as predetermined by the managers. This results in an inevitable increase in departure delays for the controlled CAVs, but it also reduces the total travel time of the mixed traffic system.

In order to minimize the average travel time of the mixed traffic system, the optimal solution will be chosen by Equation (6):

$$\left(t_{eTD}^{1*}, t_{eTD}^{2*}, \dots, t_{eTD}^{j^*}, \dots, t_{eTD}^{(|J_{in}^*| + |J_{mid}^*| + |J_{out}^*|)} \right) = \operatorname{argmin} \phi, \tag{6}$$

where $t_{eTD}^{j^*}$ represents the extra departure delay for the controlled CAV j^* , $j \in \{J_{in}^*, J_{mid}^*, J_{out}^*\}$. J_{in}^* , J_{mid}^* , and J_{out}^* is the set of CAVs controlled in each layer, respectively. $|J_{in}^*| + |J_{mid}^*| + |J_{out}^*|$ represents the sum of the number of controlled CAVs contained in the three layers.

2.4.2. Constraint Conditions

In order to protect the personal interests of the passengers on controlled CAVs, constraints are set to prevent their entry into the traffic network from experiencing an excessive amount of additional delay.

First, as can be observed from Equation (7), the maximum value of the additional departure delay should not exceed a threshold \bar{t} , which is flexible depending on the scale of the road network:

$$\forall j^* \in \{J_{in}^*, J_{mid}^*, J_{out}^*\} \quad t_{eTD}^{j^*} \leq \bar{t}, \quad (7)$$

where $j^* \in \{J_{in}^*, J_{mid}^*, J_{out}^*\}$ denotes the controlled CAV j^* ; J_{in}^* , J_{mid}^* , and J_{out}^* are the set of CAVs controlled in each layer, respectively. The variable $t_{eTD}^{j^*}$ represents the extra departure delay for the controlled CAV j^* , and \bar{t} denotes the threshold for the extra departure delay before the trip.

Furthermore, it is crucial to comply with the spatiotemporal propagation features of traffic flow. It takes longer for vehicles driving from the outside to the congestion bottleneck. As a result, it is imperative that the controlled vehicles in the outer layer should not be permitted to depart later than those situated in the middle and inner layers. Moreover, the controlled cars in the middle layer should not be permitted to depart later than those in the inner layer. Equation (8) can be used to formulate this constraint:

$$\begin{aligned} \max_{j^* \in J_{out}^*} (t_{IT}^{j^*} + t_{eTD}^{j^*}) &\leq \max_{k^* \in J_{mid}^*} (t_{IT}^{k^*} + t_{eTD}^{k^*}) \\ \max_{k^* \in J_{mid}^*} (t_{IT}^{k^*} + t_{eTD}^{k^*}) &\leq \max_{l^* \in J_{in}^*} (t_{IT}^{l^*} + t_{eTD}^{l^*}), \end{aligned} \quad (8)$$

where j^* , k^* , and l^* all denote the controlled CAVs, which belong to different layers; J_{in}^* , J_{mid}^* , and J_{out}^* are the set of CAVs controlled in each layer, respectively. The variable $t_{eTD}^{j^*}$ represents the extra departure delay for the controlled CAV j^* ; and $t_{IT}^{j^*}$ represents the desired departure time before the control for the controlled CAV j^* .

2.4.3. Computational Method

For combinatorial optimization problems, two types of solution algorithms exist: exact algorithms and heuristic algorithms [46]. Although exact algorithms can produce optimal solutions with great precision and are more suited for handling straightforward problems, they do have limitations. It tends to be difficult to acquire the best answer using exact algorithms for complicated issues with many cases. Conversely, heuristic algorithms like Genetic Algorithm (GA), Particle Swarm Optimization (PSO), Tabu Search (TS), Ant Colony Optimization (ACO), and Genetic Search (TS) can efficiently identify approximations for problems with challenging search spaces. The chosen algorithm in this work involves the use of heuristic algorithms to tackle the given model. This decision is based on the fact that the optimization problem of controlling a mixed transportation system is a non-deterministic Polynomial-hard (NP-hard) problem, making it impractical to solve using exact algorithms.

Genetic algorithms are capable of retaining and improving the best solutions in each generation by modeling the process of biological evolution and progressively converging to the global optimum. Due to this adaptation, the genetic algorithm is able to conduct a comprehensive exploration of the search space, thereby avoiding premature convergence to local optima and preserving solution diversity. The crossover and mutation procedures enable the introduction of new solutions into the search space, increasing the possibility of thoroughly exploring various places. Since GA is naturally parallel, it can evaluate

and refine several potential solutions simultaneously. It is well-suited for implementation in distributed, cloud, or multi-core computing environments, thus expediting the whole solution process. Furthermore, it has been observed that GA can work effectively in complicated contexts and is robust to the presence of noise, uncertainty, and non-convex functions in the problem [47–49].

GA has been widely used in the field of transportation [50,51], especially in solving complex, multi-objective, and real-time demanding problems, and it is a powerful tool for traffic management and planning. In the instance of the NP-hard optimization problem for managing mixed traffic systems, the genetic algorithm is selected as the solution algorithm based on the characteristics of the active control problem, the algorithm's performance, and the availability of computational resources. Table 2 presents the values of the fundamental parameters of the genetic algorithm utilized in the research.

Table 2. The values of the fundamental genetic algorithm parameters.

Parameter	Value
Pop Size	20
Generation Size	30
Crossover Probability	0.6
Mutation Probability	0.1
Elite	True

3. Simulation Results and Discussion

In this section, we report the results of our simulation-based evaluation of the traffic demand management system generated from the Network-Level Hierarchical Bottleneck Congestion Control Method.

Due to a limited number of AVs already operating on real-world road networks, even in the case of AVs that have been tested in open road environments, their average speed and headway are relatively low [25] and they still do not reach Level 5 [52]. Moreover, the application of CAVs to real-world road networks is presently limited to bound testing environments. The amount and quality of relevant traffic data that can be collected is quite restricted, and there are very few devices enabling CAVs communication on the roadways. Most of the research that has already been conducted uses simulation to evaluate traffic conditions with CAVs included. Consequently, in order to verify the efficacy of the proposed model, experiments were carried out on two distinct networks of varying scales in Shanghai using the simulation program Simulation of Urban MObility (SUMO). Figure 3 shows the topology of two networks. We evaluate the efficacy of this method using various road network sizes, different penetration rates of CAVs, and different proportions of the controlled CAVs.

Table 3 contains some of the fundamental parameter configurations for HDVs and CAVs within the simulation. The following model of the CAVs is chosen to be the cooperative adaptive cruise control (CACC) [53–56] model, which has been validated by PATH Laboratory at the University of California, Berkeley. Moreover, the widely used Intelligent Driver Model (IDM) [45] is selected as the HDVs following the model in this study.

In this study, the GA known for its fast-computational speed was selected to solve the developed model. In order to make the extra delay for CAVs not too long, the solution precision was set to 1 min and $\bar{t} = 5$ min, thus $0 \leq eTD_{j^*} \leq 5$ min, $j^* \in \{J_{in}^*, J_{mid}^*, J_{out}^*\}$. Therefore, the delay range was divided into six different values. Each chromosome in the GA had a length of three, representing the three control layers.

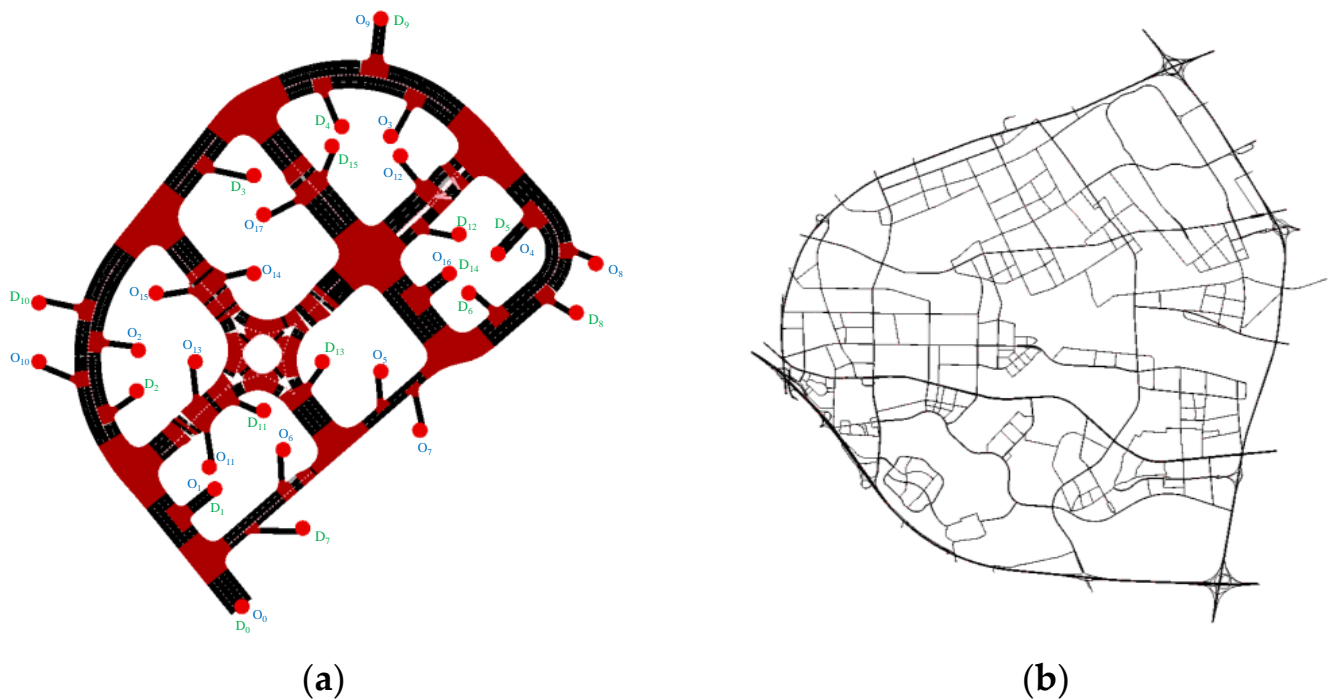


Figure 3. The topology of two networks: (a) Small-scale network; (b) large-scale network.

Table 3. The simulation's basic parameter settings for HDVs and CAVs.

Parameter	HDVs	CAVs
Minimum gap (m)	2.5	1.5
Acceleration (m/s^2)	2.6	2.6
Deceleration (m/s^2)	4.5	4.5
Emergency deceleration (m/s^2)	9	9
Car following model	Intelligent driver model (IDM)	Cooperative adaptive cruise control (CACC)

3.1. Small-Scale Network with Different CAVs' Penetration Rates

Figure 3a depicts the road network topology for the closed road scenario, which is a more typical surface road area. The small-scale square-like road network has a more uniform distribution. The network consists of eight traffic light intersections, one roundabout, eighteen entries, sixteen exits, and spans approximately 500 m by 500 m in total area.

3.1.1. A total of 50% CAVs' Penetration Rate

In our earlier publication [57], we analyzed and simulated three different scenarios pertaining to the OD distribution in a small-scale road network. These scenarios include Scenario I, which represents a relatively uniform OD distribution; Scenario II, characterized by a “near-low-far-high” OD distribution; and Scenario III, featuring a “near-high-far-low” OD distribution. The analysis was conducted using a 50% penetration rate of CAVs. In each scenario, the congestion bottleneck is identified, and the relevant layers are divided. The optimal control optimization scheme is then determined using GA. To access further details on the three scenarios, readers are advised to refer to the paper [57].

The average departure delay before travelling \bar{t}_{DD} , the travel duration in the network \bar{t}_{TD} , the average travel time, and the objective function ϕ before and after the control optimization are compared. The control effects of three scenarios of OD distribution for this small-scale road network under a 50% CAV penetration rate are shown in Table 4.

Table 4. The control effects of three scenarios of OD distribution for this small-scale road network under 50% CAVs' penetration rate.

Evaluation Indicators	Scenario I			Scenario II			Scenario III		
	Before Control (s)	After Control (s)	Improvement (%)	Before Control (s)	After Control (s)	Improvement (%)	Before Control (s)	After Control (s)	Improvement (%)
Controlling vehicles proportion	-	2.71%	-	-	4.35%	-	-	5.53%	-
$\sum_{j^* \in \text{CAVs}} t_{eTD}^{j^*}$	-	4020	-	-	5940	-	-	7620	-
\bar{t}_{DD}	229.18	153.51	33.02	350.47	32.38	90.76	435.65	283.99	34.81
\bar{t}_{TD}	327.53	98.81	69.83	332.18	161.95	51.25	246.26	208.09	15.50
Average travel time	556.71	252.32	54.68	682.65	194.33	71.53	681.89	492.08	27.84
ϕ	556.71	257.05	53.83	682.65	201.32	70.51	681.89	501.04	26.52

It may be inferred that the recommended control method performs well in various OD distribution scenarios and holds potential utility for small-scale networks. The optimal control effect is observed in the OD distribution scenario II, characterized by a “near-low-far-high” pattern. Subsequently, the OD distribution scenario I, which exhibits a nearly uniform distribution, demonstrates a somewhat favorable control effect. Moreover, the OD distribution scenario III, characterized by a “near-high-far-low” pattern, exhibits the least desirable control effect. In the least-favorable scenario, the average travel time is also lowered by more than 25%. Furthermore, all these scenarios exhibited a decrease in both temporal and spatial extent of congestion throughout the road network, demonstrating the high effectiveness of the control method.

Further experimentation is necessary to validate the effectiveness of the suggested network-level hierarchical bottleneck congestion control method.

3.1.2. Different CAVs' Penetration Rates

Based on the congested bottleneck and three control layers found at Scenario I, a simulation analysis was conducted under various CAVs' penetration rates to confirm the applicability of the proposed method. To guarantee consistency between varying penetration rates, the overall simulation time for every scenario was maintained at around 3500 s. Table 5 displays the settings for the simulated experiments for the penetration rates as well as the three parameters \bar{t}_{DD} , \bar{t}_{TD} , and average travel time before control.

Table 5. Traffic demand and parameter values before control for each CAVs' penetration rate.

CAVs' Penetration Rate	Traffic Demand (pcu/1800 s)	Total Simulation Time (s)	Average Depart Delay \bar{t}_{DD} (s)	Average Travel Duration \bar{t}_{TD} (s)	Average Travel Time (s)
10%	740	3430	108.96	399.83	508.79
20%	730	3429	136.03	265.36	401.39
30%	825	3656	105.33	315.57	420.90
40%	900	3319	140.02	305.78	445.80
50%	850	3658	229.18	327.53	556.71
60%	900	3575	265.60	399.06	664.66
70%	975	3429	175.91	270.88	446.79
80%	1150	3562	251.57	240.34	491.91
90%	1230	3433	169.89	202.21	372.10
100%	1500	3698	192.29	164.97	357.26

Table 5 shows that, barring a few instances, there was a positive correlation between the penetration rate of CAVs and the capacity of the road network to accommodate vehicle traffic. This observation holds true when considering a comparable duration of the simulation period. The use of both the congestion bottleneck and the three control layers that were set up at the 50% penetration rate remains. By employing GA, the optimal regulation schemes were identified for each penetration rate. Table 6 and Figure 4 present the effectiveness of the traffic system under the corresponding optimal regulatory schemes at various levels of penetration.

Table 6. The control effectiveness at different CAVs’ penetration rates.

CAVs’ Penetration Rate (%)	ϕ before Control (s)	Proportion of Controlled CAVs (%)	$\sum_{j \in \text{CAVs}} t_{eTD}^j$	ϕ after Control (s)	Improvement of ϕ (%)
10	508.79	0.27	7	260.57	50.05
20	401.39	0.96	20	391.27	7.09
30	420.90	1.82	32	249.75	47.71
40	445.80	2.11	54	323.46	38.75
50	556.71	2.71	61	300.85	56.14
60	664.66	3.78	114	636.66	20.22
70	446.79	3.90	84	349.49	39.42
80	491.91	4.17	107	454.68	28.19
90	372.10	6.26	231	464.54	34.21
100	357.26	3.40	126	416.43	17.30

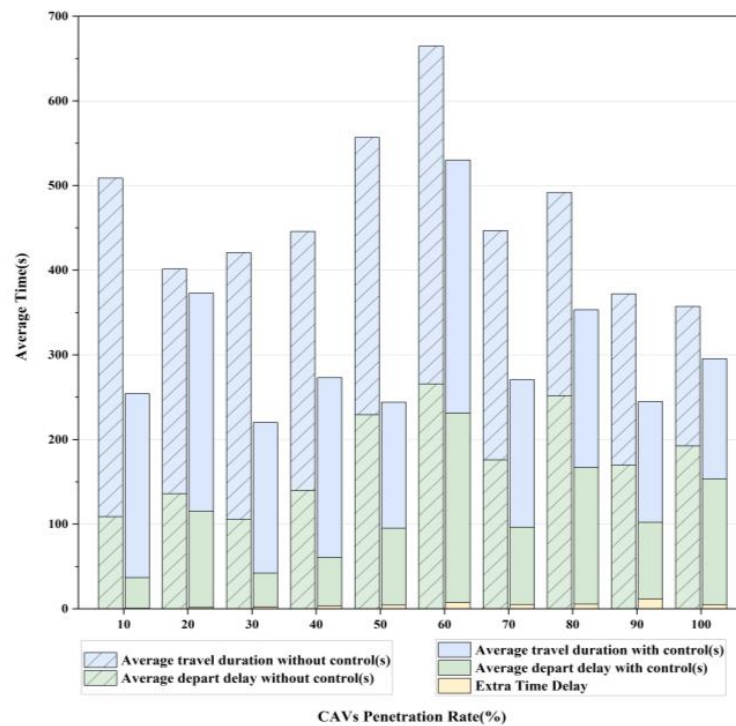


Figure 4. The comparison of congestion control effectiveness under different CAVs’ penetration rates.

The method proposed in this paper is characterized by its simplicity and efficacy in controlling the propagation of congestion. The highest performance was achieved when the penetration rate of CAVs reached 50%, while the least favorable performance was recorded at a penetration rate of 20%. The variations in penetration rates of CAVs have a direct impact on the congestion bottlenecks and corresponding layers across the entirety of the road network. However, the recalculation of congestion bottlenecks and their corresponding layers is not conducted at different penetration rates, resulting in less efficient control

measures at other penetration rates. Therefore, in order to determine the optimal traffic demand regulation scheme, it is imperative to obtain congestion bottlenecks and layers that correspond to different CAVs' penetration rates. Implementing traffic demand regulation without identifying congestion bottlenecks does not lead to optimal control.

3.2. Large-Scale Network under Different Proportions of Controlled CAVs

The magnitude of real-world transportation road networks is substantial. So, we have undertaken simulation investigations on large-scale road networks to validate the practicality of the method proposed in this paper for real-world implementation. The large-scale network comprises a total of 2022 entrances and is encompassed within a spatial expanse measuring $15,000 \times 15,000$ m. These entrances are categorized into 67 TAZs. The initial traffic demand for the simulation in this network is derived from the real-time traffic data that was gathered.

The average travel duration per vehicle on the network is about 935.96 s and the average departure delay before the trip is approximately 2.04 s when traffic volumes are low and vehicles are moving freely.

3.2.1. 50% CAVs' Penetration Rate

The control model was initially developed and evaluated with regards to a 50% penetration rate for CAVs. During a time span of 1800 s, a total of 21,085 vehicles were introduced into the existing road network. At this point, there exists a significant level of traffic congestion, resulting in a prolonged overall simulation time of 15,360 s.

The average travel duration \bar{t}_{TD} for each vehicle is 2381.45 s, with an average departure delay \bar{t}_{DD} of 109.95 s per vehicle before the implementation of control measures. It is noted that the total analysis time T_{\max} , i.e., the maximum value of $t + T_{\text{interval}}$, can be determined using Equation (9):

$$T_{\max} = t_{\text{insert}} + \bar{t}_{TD} + \bar{t}_{DD} = 1800 + 2381.45 + 109.95 = 4291.4 \text{ s}, \quad (9)$$

where t_{insert} is the total duration of traffic input into the road network. Since in this scenario vehicles are imported into the simulation for only 1800 s, no subsequent vehicles are newly input into the road network; $t_{\text{insert}} = 1800$ s.

- Congestion bottleneck and control layers;

The spatially averaged vehicle speeds for each road edge under $T_{\text{interval}} = 900$ s are calculated based on the simulation output. The number of times that the spatially averaged speed of the road edge numbered 424217529#0 went below the critical speed v^* was 15, which is the most frequent of all road edges. Thus, the congestion bottleneck numbered 424217529#0 was identified, which corresponds to the target time $T^* = 1350$ s for congestion control, after which the congestion gradually spreads out across the road network. Set $t_0 = 450$ s, and the time period for implementing control measures is $T_{\text{control}} = [0, 1350]$ s. The time periods for the implementation of control measures in each layer are $T_{\text{out,control}} = [0, 450)$ s for the outer layer, $T_{\text{mid,control}} = [450, 900)$ s for the middle layer, and $T_{\text{in,control}} = [900, 1350)$ s for the inner layer. Moreover, the roadway edges beyond the bottleneck were divided into layers, setting $l_0 = 5000$ m. The respective positions are depicted in the Figure 5.

Based on this, the CAVs in the corresponding time period of the three layers were controlled. The number of vehicles in the set of controlled vehicles in each layer during the time period in which the control measures were implemented was $|J_{\text{in}}^*| = 452$, $|J_{\text{mid}}^*| = 1369$, and $|J_{\text{out}}^*| = 263$, respectively. The total number of CAVs that can be controlled is 2084, which is 9.88% of the total number of vehicles on the road network.

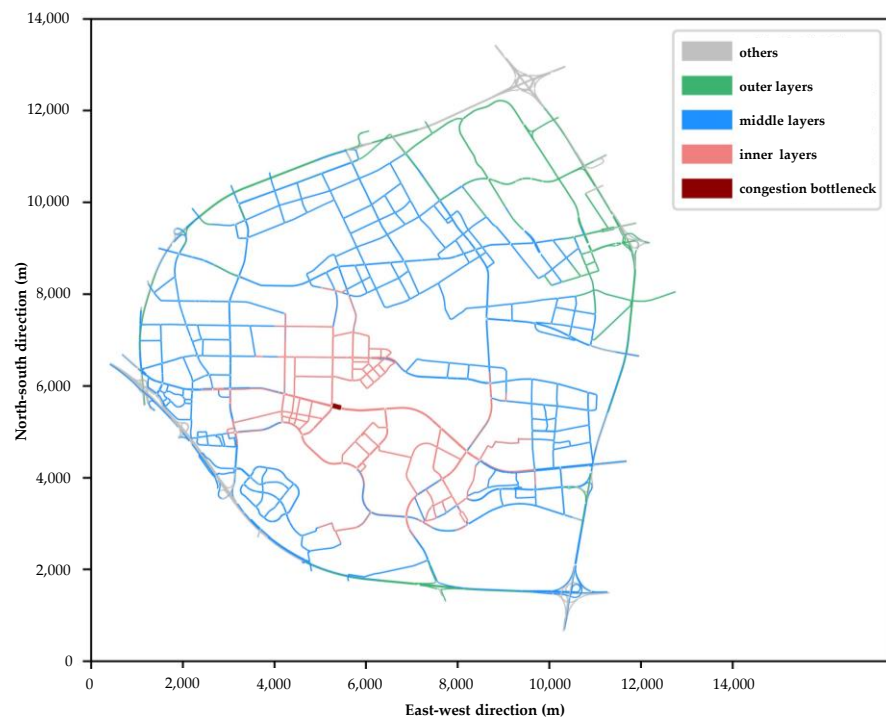


Figure 5. The corresponding locations of the congested bottleneck and layers on the large-scale network.

- Optimal regulation scheme of traffic demand.

Figure 6 depicts the utilization of GA to minimize the objective function and explore the solution set in the context of a scenario, where there is a 50% CAVs’ penetration on a large-scale road. The optimal traffic demand regulation scheme corresponding to making the objective function obtain the minimum value is obtained.

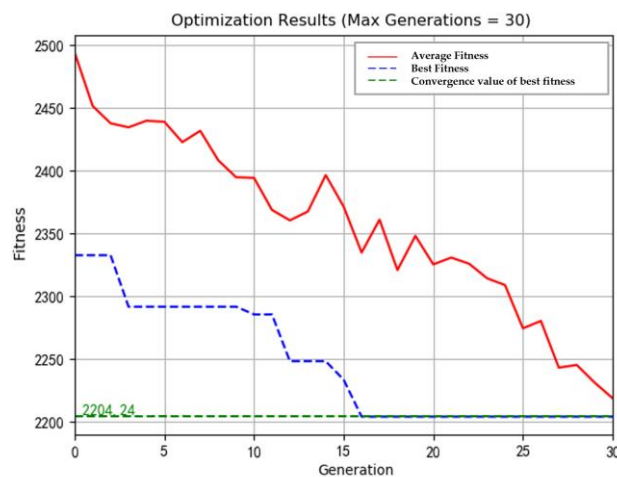


Figure 6. The search process of the GA for the large-scale road network.

- Control effectiveness;

The average departure delay before travelling \bar{t}_{DD} , the travel duration in the network \bar{t}_{TD} , the average travel time and the objective function ϕ before and after the control optimization are compared, and the comparison results are shown in the Table 7.

Table 7. The control effects of large-scale road networks at 50% penetration of CAVs.

Evaluation Indicators	Free Flow (s)	50% CAVs Penetration Rate		
		Without Control (s)	With Control	
			Value (s)	Compare to without Control (%)
\bar{t}_{DD}	2.04	103.95	101.96	1.91
\bar{t}_{TD}	935.96	2381.45	2087.58	12.34
Average travel time	938.00	2485.40	2189.54	11.90
$\sum_{j^* \in \text{CAVs}} t_{eTD}^{j^*}$	-	-	309,900	-
ϕ	938.00	2485.40	2204.24	11.31

The most effective traffic demand regulation scheme is capable of managing approximately 9.88% of the total vehicles within the large-scale road network. As a result, there is a notable decrease in the average travel time of the vehicles by 11.90% and a corresponding reduction in the value of the objective function by 11.31%. However, the improvement shown in a small-scale road network is comparatively more substantial, as it exhibits an average travel time reduction exceeding 50%. The explanation could be that there are multiple bottlenecks in large-scale road networks. To achieve enhanced control, it becomes necessary to handle each bottleneck independently.

To conduct a more comprehensive evaluation of the efficacy of the control method, this study aims to delve into further detail. The speed and time indicators provided below are intended for analysis.

1. Time indicators.

The time indicators for the road network and TAZs are expressed in terms of spatially averaged travel times. The following is a description of the calculation procedure.

The spatially average travel time $\bar{T}_{[t,t+T_{\text{interval}}]}^{\text{taz}_k}$ of the TAZ taz_k over the time period $[t, t + T_{\text{interval}})$ is calculated from the spatially average travel time $\bar{T}_{[t,t+T_{\text{interval}}]}^{e_j}$ of the road edge e_j over the time period $[t, t + T_{\text{interval}})$. Considering that the length of each road edge is different, the calculation needs to be weighted according to the length of the road edges and calculated using the Equation (10):

$$\bar{T}_{[t,t+T_{\text{interval}}]}^{\text{taz}_k} = \frac{\sum_{e_j \in \text{taz}_k} \bar{T}_{[t,t+T_{\text{interval}}]}^{e_j} / \frac{l_{e_j}}{\bar{l}}}{N_{\text{taz}_k}}, \quad (10)$$

where $\bar{T}_{[t,t+T_{\text{interval}}]}^{e_j}$ denotes the spatially average travel time of the road edge e_j over the time period $[t, t + T_{\text{interval}})$ can be calculated by the Equation (2). \bar{l} is the average length of all edges included in the road network, $\bar{l} = \frac{\sum_{j \in \{1,2,\dots,N_{\text{edges}}\}} l_{e_j}}{N_{\text{edges}}}$. N_{edges} is the total number of edges in the road network. l_{e_j} is the length of edge e_j .

The spatially average travel time \bar{T}_{taz_k} for TAZ taz_k is finally calculated using Equation (11):

$$\bar{T}_{\text{taz}_k} = \frac{\bar{T}_{[t,t+T_{\text{interval}}]}^{\text{taz}_k}}{n}, \quad (11)$$

where n denotes the number of time periods with time interval T_{interval} included in the total analysis time T_{max} and can be calculated by the Equation (3).

What is more, the spatially average travel time \bar{T} of the road network is also calculated, first using Equation (12) to calculate the spatially average travel time $\bar{T}_{[t,t+T_{\text{interval}}]}$ of the road network over the time period $[t, t + T_{\text{interval}}]$.

$$\bar{T}_{[t,t+T_{\text{interval}}]} = \frac{\sum_{e_j} \bar{T}_{[t,t+T_{\text{interval}}]}^{e_j} \cdot \frac{l_{e_j}}{\bar{T}}}{N_{\text{edges}}} \quad (12)$$

This is then averaged over time and calculated using Equation (13) to obtain the spatially average travel time \bar{T} for the entire road network:

$$\bar{T} = \frac{\sum_{t \in \{0, T_{\text{interval}}, \dots, (n-1)T_{\text{interval}}\}} \bar{T}_{[t,t+T_{\text{interval}}]}}{n} \quad (13)$$

2. Speed indicator.

The speed indicator is expressed as the spatially averaged vehicle speed $\bar{v}_{[t,t+T_{\text{interval}}]}^{\text{layer}}$ over the time period $[t, t + T_{\text{interval}}]$, where $\text{layer} \in \{\text{in, mid, out, bottleneck}\}$. Using calculations, Equation (14) also needs to be weighted according to the length of the edge:

$$\bar{v}_{[t,t+T_{\text{interval}}]}^{\text{layer}} = \frac{\sum_{e_j \in \text{layer}} \bar{v}_{[t,t+T_{\text{interval}}]}^{e_j} \cdot \frac{l_{e_j}}{\bar{T}}}{N_{e_j \in \text{layer}}}, \quad (14)$$

where $\bar{v}_{[t,t+T_{\text{interval}}]}^{e_j}$ can be calculated by the Equation (4), $N_{e_j \in \text{layer}}$ denotes the number of road edges included in the layer.

This is then averaged over time and calculated using Equation (15) to obtain the spatially average vehicle \bar{v}_{layer} for each layer:

$$\bar{v}_{\text{layer}} = \frac{\sum_{t \in \{0, T_{\text{interval}}, \dots, (n-1)T_{\text{interval}}\}} \bar{v}_{[t,t+T_{\text{interval}}]}^{\text{layer}}}{n}, \quad (15)$$

where n denotes the number of time periods with time interval T_{interval} included in the total analysis time T_{max} , which can be calculated by the Equation (3).

3. Calculation results of the indicators.

The effectiveness of the best traffic demand regulation scheme at 50% CAVs' penetration under the large-scale roads is evaluated. Set $T_{\text{interval}} = 900$ (s). The equations discussed earlier are used to calculate the spatially average travel time of each TAZ both before and after the control, as indicated in Figure 7. Additionally, it calculates the ratio between the spatially average travel time in the free-flow and the spatially average travel time of each TAZ both before and after the control.

To provide additional elucidation on the control impact of TAZs at different locations, Figure 8 displays the ratio values in Figure 7b,c, which correspond to the locations of the TAZs. The figure displays the location and shape of each TAZ. The values assigned to the areas indicate the corresponding ratios. Figure 8b shows the color representation of each area at the bottom, indicating whether there was an improvement in the spatial average travel time after the control. The color green is indicative of improvement, while a yellowish color suggests little change, and the color orange indicates degradation.

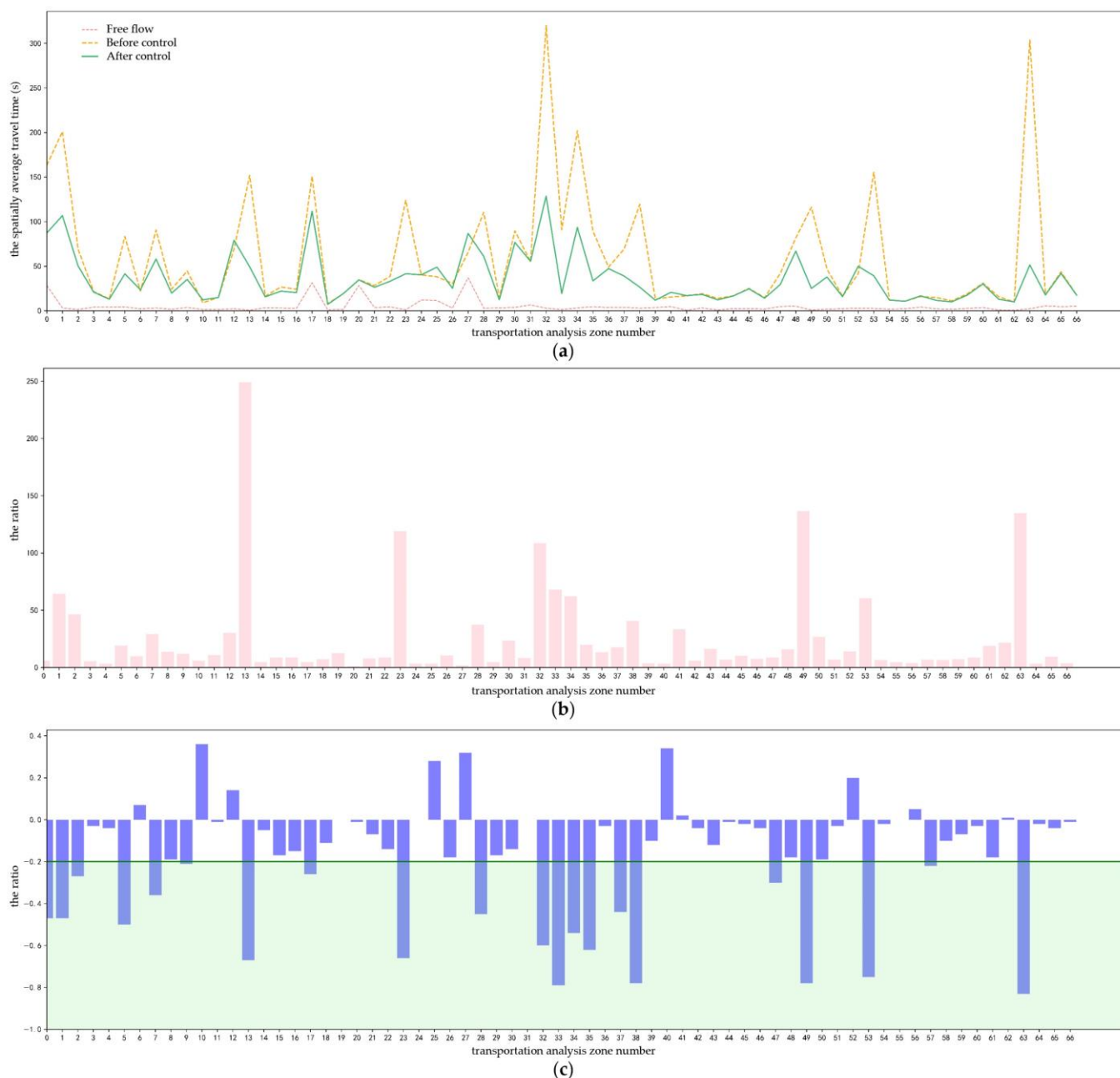


Figure 7. (a) The spatially average travel time of each TAZ in free flow, before control and after control; (b) the ratio of the spatially average travel time of each TAZ before control to the spatially average travel time under free flow; (c) the ratio of the spatially average travel time of each TAZ after control to the spatially average travel time under free flow.

As indicated by Figures 7b and 8a, the congestion condition is extremely terrible before control. On the other hand, the results depicted in Figures 7c and 8b demonstrate a significant improvement in traffic efficiency within the majority of TAZs, and traffic efficiency has greatly increased when employing the optimal control scheme derived from the control method suggested in this work. The implementation of this method has led to a decrease in travel time in 57 TAZs, accounting for over 85% of the overall TAZs' count. Notably, in 19 TAZs, or 28.36% of the total TAZs, the improvement in travel time exceeds 20%.

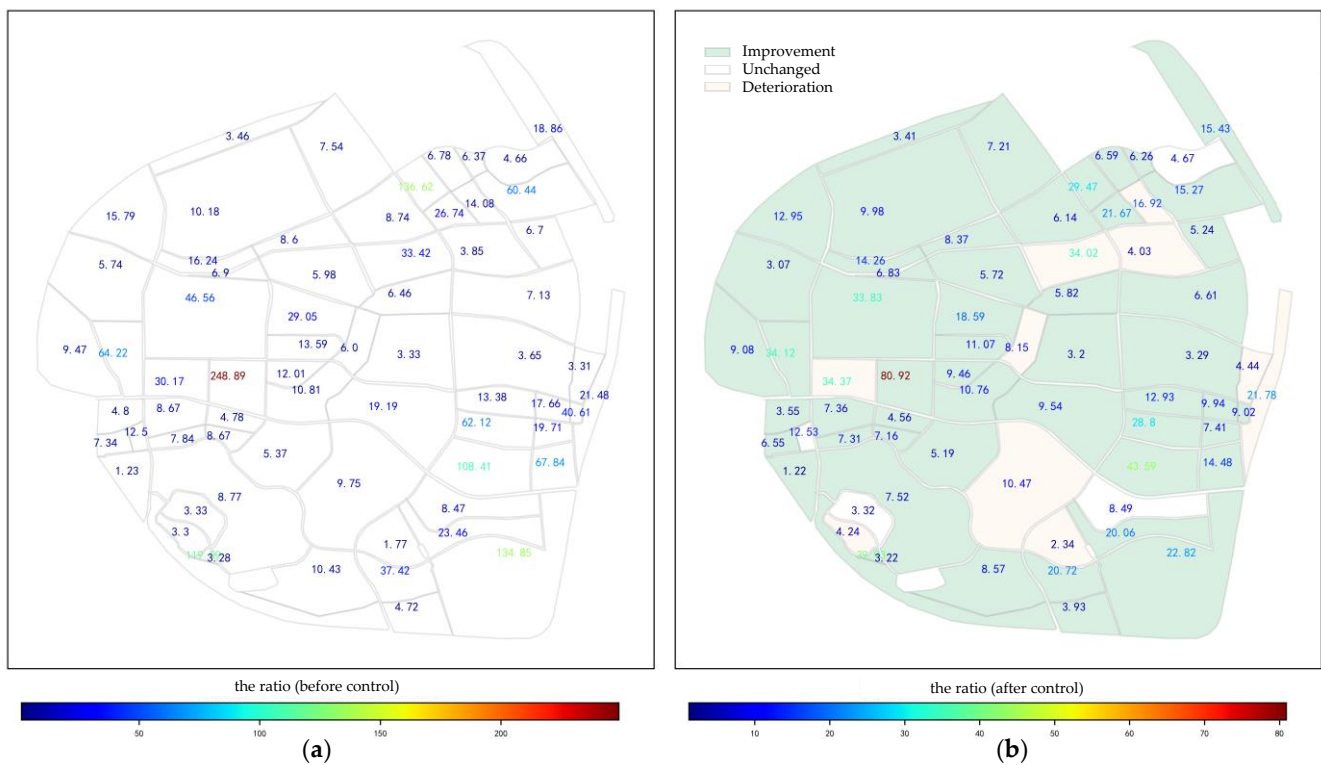


Figure 8. (a) Map of the ratio of spatially averaged travel time for traffic TAZs (before control); (b) map of the ratio of spatially averaged travel time for traffic TAZs (after control).

As for the spatially average travel time of the whole road network: In the free flow condition, the spatially average travel time was 4.58 s. Prior to implementing control optimization, the spatially average travel time was significantly higher at 58.25 s, resulting in a ratio of 12.72 times the free flow. However, after control optimization, the spatially average travel time decreased to 35.03 s, resulting in a ratio of 7.65 times the free flow condition. The observed increase in the spatially average travel time between the before and after control amounted to 39.86 (%). The study provides additional confirmation of the effectiveness of the active control method through the analysis of spatial average travel time indicators. This method has the potential to greatly enhance traffic conditions by effectively controlling a limited number of CAVs at the road network level.

After that, the speed indicator was calculated and analyzed. Equation (11) is used to calculate the regionally averaged speed over time for each layer and bottleneck, resulting in the presentation of these data in Figure 9.

Then, Equation (12) was used to obtain the spatially averaged vehicle speeds for each layer, both before and after the control. The results are displayed in Table 8.

Following the implementation of the control, the spatial average speeds at the bottleneck and layers are significantly improved. The most substantial improvement is observed at the congestion bottleneck, where the average speed experiences a remarkable increase of about 30%.

Table 8. Comparison of spatially average vehicle speeds before and after control.

	Bottleneck	Inner Layer	Middle Layer	Outer Layer
Before control (km/h)	10.0	8.22	11.15	19.75
After control (km/h)	12.86	8.82	11.87	20.40
Improvement (%)	28.60	7.30	6.46	3.29

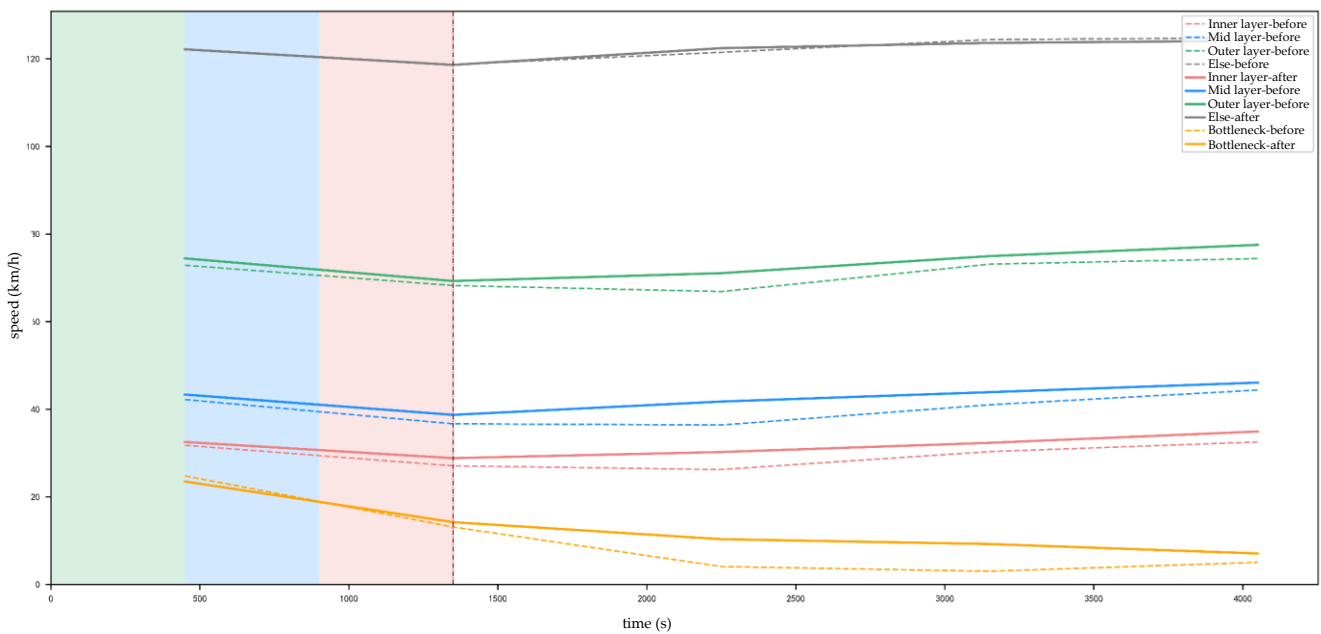


Figure 9. The regionally averaged speed over time for each layer and bottleneck.

To obtain the data in Table 9, the process involves integrating the average vehicle speed during a specific time period. This integration is performed by calculating the area enclosed by the X-axis, and the curves represented spatially averaged vehicle speeds, as depicted in Figure 9.

Table 9. Comparison of area of the region bounded by the X-axis and the spatially averaged vehicle speeds curves before and after control.

	Bottleneck	Inner Layer	Middle Layer	Outer Layer
Before control (km)	8.77	28.93	39.33	70.45
After control (km)	12.26	31.27	42.46	72.81
Improvement (%)	39.79	8.09	7.45	3.35

The area enclosed by the X-axis and the spatial average speeds curves at the congestion bottleneck and each layer are significantly larger after control. This observed physical quantity increases more than 40% within the congestion bottleneck, where the improvement is particularly noticeable.

Table 10 presents the outcomes derived from the computation of the duration of the speed reduction, which refers to the period during which the slope of the curve exhibits negativity. This calculation is based on the data provided in Figure 9.

Table 10. Comparison of the duration of speed reduction before and after control.

	Bottleneck	Inner Layer	Middle Layer	Outer Layer
Before control (h)	0.38	0.25	0.25	0.25
After control (h)	0.50	0.12	0.12	0.12
Improvement (%)	−31.58	52.00	52.00	52.00

The duration of speed reduction at each layer experiences a significant decrease of over 50% following the implementation of control, despite the fact that the duration at the bottleneck remains extended. The spatially averaged vehicle speeds in each layer are reduced only during the implementation time period, and $T_{\text{control}} = [0, 1350 \text{ s}]$ of the control, after which the speeds continue to increase.

Furthermore, Figure 10 presents a thermogram depicting the spatial average vehicle speed improvement for each roadway edge during a specific time period. This visualization aims to further elucidate the comparison between spatial average vehicle speeds before and after the control, across various time periods and roadway edges. Figure 10a,b present the thermograms illustrating the improvements in speed over the time intervals of 900–1800 s and 3600–4500 s, respectively. The lines depicted in the graphs represent the road edges, and the color of the road edge corresponds to the magnitude of the speed improvement percentage. A bluer color signifies a more significant improvement in speed, while the redder color indicates a decline in speed after control.

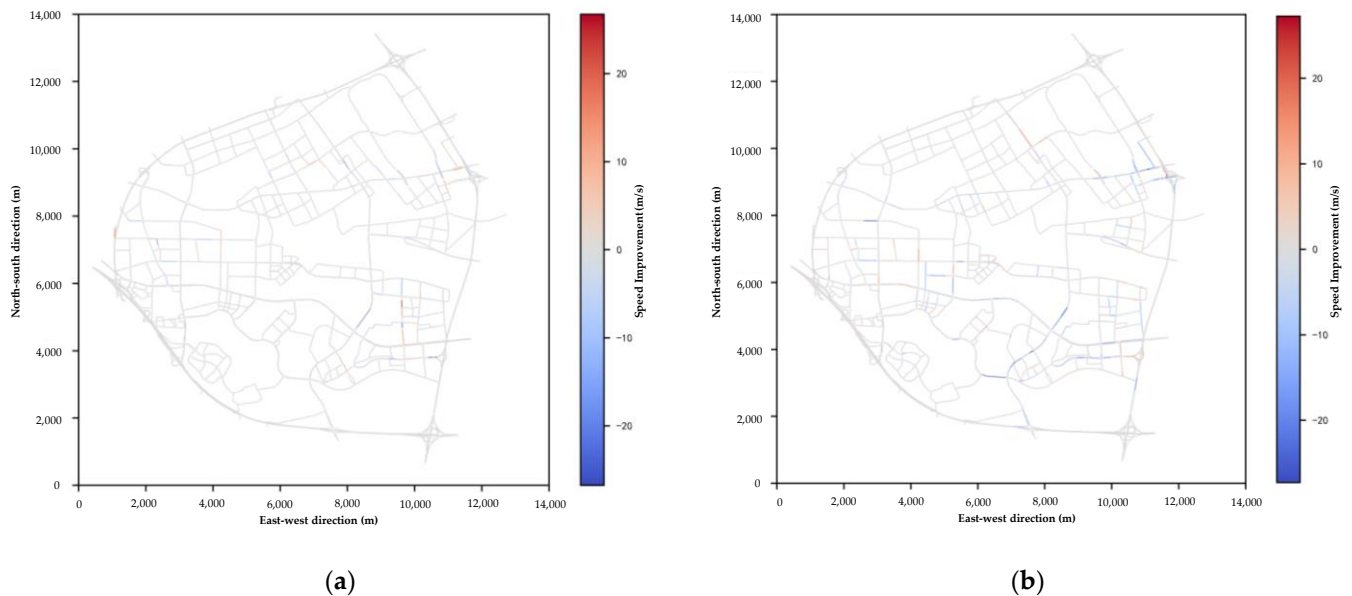


Figure 10. Thermograms of the speed improvement on the road network before and after the control: (a) from 900 (s) to 1800 (s); (b) from 3600 (s) to 4200 (s).

The data presented in Figures 9 and 10 indicate that the implementation of traffic demand regulation does not yield rapid improvements in the traffic conditions of the road network. The propagation of optimization resulting from regulation must progressively disseminate across the network, similar to the spread of congestion.

Furthermore, it can be inferred from Tables 8–10 that there exists a positive correlation between the proximity of edges to the congestion bottleneck and the quality of control performance. Generally speaking, the traffic bottleneck experiences the greatest improvement, resulting in a reduction in both the spatial and temporal extent of the traffic congestion it causes and propagates. The control strategy proposed in this research efficiently achieves our goal of managing traffic congestion at the bottleneck and subsequently managing the traffic condition over the entire road network.

To summarize, this paper presents a preliminary verification of the effectiveness of the control method proposed for large-scale road networks. Although the increase in the objective function value is less significant in the case of large-scale road networks, there is a notable improvement in the calculated time and speed indicators. Specifically, there is a considerable improvement in the indicators at the congestion bottleneck.

3.2.2. Comparison with Dynamic User Equilibrium Scheme

The effectiveness of the control method proposed in this paper is further verified by comparing the simulation results with the route choice results obtained from Dynamic User Equilibrium (DUE) model. DUE account for the dynamics of traffic flow. When travelers select their path to minimize their own journey time, it is utilized to characterize the status of a traffic network [58,59].

In our analysis, we conducted an extensive comparison of the route choices provided by DUE, while maintaining the initial traffic demand and a consistent penetration rate of 50% CAVs. The (approximate) user dynamic equilibrium was calculated using the dualIterate.py tool in the SUMO software. The average departure delay before travelling \bar{t}_{DD} , the average travel duration in the network \bar{t}_{TD} , and the objective function value $\phi = \bar{t}_{DD} + \bar{t}_{TD}$ of 100 iterations are shown in Figure 11.

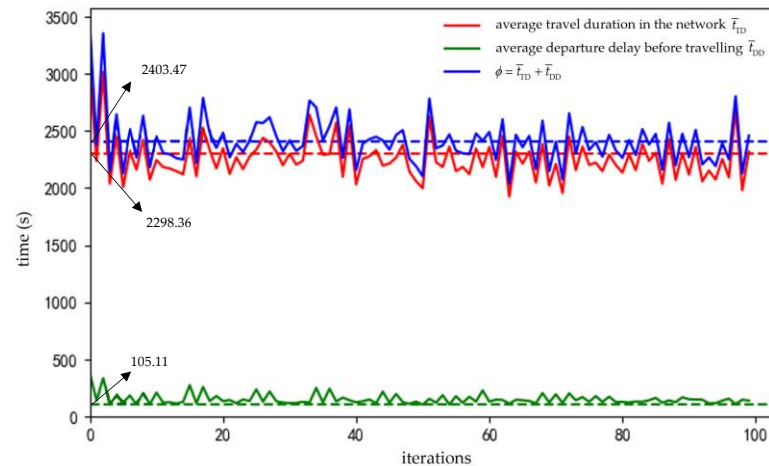


Figure 11. The three parameters for 100 iterations of the DUE simulation.

The experimentation involved the utilization of a 12th Gen Intel(R) Core (TM) i9-12900KF central processing unit (CPU). The convergence criteria were met after doing over 100 repetitions, requiring a duration exceeding 24 h. The outcomes derived by the optimal control technique in Section 3.2.1 are compared with the result of the 63rd iteration out of these 100 iterations, wherein the minimum objective function value ϕ is achieved. Table 11 displays the outcomes of the comparison.

Table 11. Comparison of the results of the proposed control method and DUE.

Evaluation Indicators	Control Method Proposed in This Study	DUE
\bar{t}_{DD} (s)	101.96	113.00
\bar{t}_{TD} (s)	2087.58	1925.68
ϕ (s)	2204.24	2038.68
Approximate compute duration (h)	12	26

It can be concluded that the route choice results obtained from DUE in a more significant reduction in average travel duration \bar{t}_{TD} as well as an objective function value of ϕ when compared to the control method provided in this paper. Nevertheless, there is an increase in the vehicle's average delay before vehicles entering the road network becomes longer. Furthermore, compared to the method in this paper, the process of employing the DUE iteration for identifying the route choosing system necessitates a much greater amount of computational time. Moreover, the method in this paper only needs to manage a limited number of CAVs, and also exhibits a favorable applicability and maneuverability in comparison to DUE. In addition, the implementation of DUE in real road networks poses challenges due to the need for comprehensive control over all vehicles inside the network to determine their travel route, which is practically impossible in practical applications.

3.2.3. Different CAVs' Control Proportions

While the proportion of vehicles subject to regulation in the small-scale road network stands at 2.71%, the corresponding figure for controlled Connected Autonomous cars

(CAVs) in the large-scale road network is 9.88%. It might be argued that these proportions of controlled CAVs does not yield a significant impact. Thus, the problem of whether traffic efficiency can also be improved by controlling a portion of the CAVs in set $\{J_{in}^*, J_{mid}^*, J_{out}^*\}$ is examined. To evaluate the extent of control effectiveness, a 50% penetration rate of CAVs was implemented on a large-scale road network. Different quantities of controlled CAVs were selected to observe the difference in effectiveness.

The only modification is the proportion of controlled CAVs. All other factors, including the initial traffic demand, the 50% CAV penetration rate, the congestion bottleneck, and the constructed divided layers established before, have stayed constant. The average departure delay before travelling \bar{t}_{DD} , the travel duration in the network \bar{t}_{TD} , the average travel time, and the objective function ϕ before and after the control optimization are compared, and the comparison results are shown in Table 12 and Figure 12.

Table 12. The control effectiveness with different CAVs' control proportion.

Serial Number	Proportion of Controlled CAVs (%)	Average Depart Delay \bar{t}_{DD} (s)	Average Travel Duration \bar{t}_{TD} (s)	$\sum_{j^* \in \text{CAVs}} \bar{t}_{eTD}^{j^*}$ (min)	ϕ (s)	Improvement of ϕ (%)	
Before control	-	-	103.95	2381.45	-	2485.40	-
After control	1	0.54	103.29	2138.63	300	2242.77	9.76
	2	2.29	104.55	2126.73	1370	2235.18	10.07
	3	4.47	102.33	2113.00	2581	2222.67	10.57
	4	6.56	100.67	2102.36	3813	2213.88	10.92
	5	9.88	101.96	2087.58	5165	2204.24	11.31

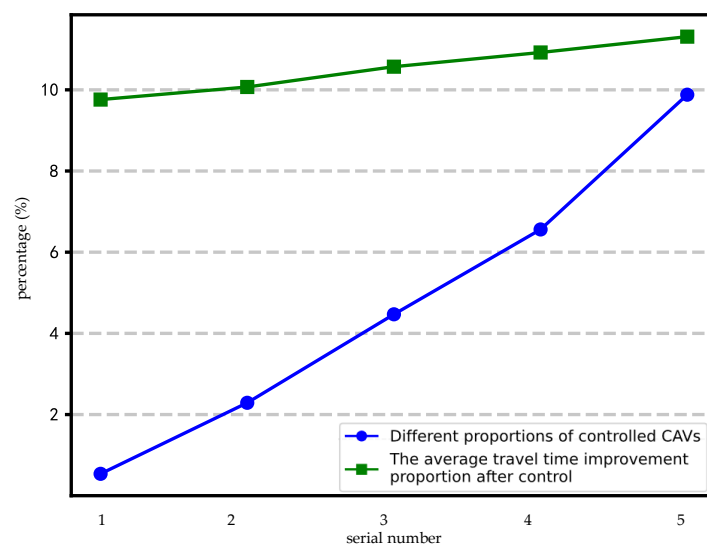


Figure 12. Comparison of congestion improvement percentages with different proportions of controlled CAVs.

In the experiment including different proportions of CAVs, it is noted that an increase in the management of CAVs or the regulation of traffic demand resulted in a more pronounced improvement in congestion management. However, the improvement in average travel time is correlated with a nonlinear fraction of controlled CAVs. The average travel time experiences a less than twofold improvement when the number of controlled connected and autonomous vehicles (CAVs) is increased by a factor of 16.

It is evident that regulating the growing number of CAVs can enhance the performance of the transportation system. However, it is crucial to evaluate the cost-effectiveness of implementing such control methods. In order to mitigate traffic congestion, it is neither

necessary nor practicable to indiscriminately regulate a substantial number of CAVs, as such would result in a considerable waste of resources. In the context of this large-scale road network, the management of a mere 0.54% of the overall vehicle demand has the potential to yield an approximate 10% reduction in average travel time.

In general, the control method produced a highly effective traffic demand management technique, which has proven to be successful at alleviating recurrent traffic bottlenecks. The road networks of varying scales, encompassing both small and large networks, substantiates the notion of control. The method exhibits the potential for application in terms of reducing travel time for travelers and enhances the overall efficiency of the road network through the management of a limited number of CAVs.

4. Conclusions

Connected and Autonomous Vehicles (CAVs), which can be effectively managed by traffic organizers, present a good prospective solution to alleviating traffic congestion. This research proposes a network-level hierarchical bottleneck congestion control method aimed at optimizing the departure time of CAVs as they access the main road through the entrance lane. In this study, a linear programming model is formulated with the objective of minimizing the average travel time of the entire mixed traffic system consisting of CAVs and HDVs. The model also incorporates restrictions to protect the individual interests of passengers in the CAVs. The optimal control scheme that satisfies the objective function and restrictions is determined through the utilization of a genetic algorithm. A simulation analysis is employed to validate the effectiveness of the control method in diverse road network sizes, CAVs penetration rates, and controlled CAVs proportions. The results demonstrate that regulating less than 3% of the quantity of CAVs in a small-scale road network can result in a minimum of 25% and maximum of nearly 70% decrease in the network's average travel time. Moreover, in a large-scale network, controlling less than 1% of CAVs can result in a nearly 10% decrease in the average journey time of the system.

Notably, in order to regulate the same roadway network with varying CAVs' penetrations, this study necessitates the dynamic identification of congestion bottlenecks and the dynamic division of the control layer in order to achieve optimal control results. Controlling a smaller number of CAVs can still increase access efficiency to a sufficient degree, whereas haphazardly regulating a large number of CAVs wastes resources. A practical control method is proposed in this study to facilitate the advancement of environmentally sustainable transportation.

The method proposed in this paper exhibits some limitations as well, including its primary emphasis on network-level traffic management. Future studies should explore the potential integration of this method with traffic control methods at the intersection- and corridor levels. It is better to implement a comprehensive integrated control system that operates at the intersection, corridor, and network levels. In the meantime, the acquisition of each CAV's scheduled departure time is a significant challenge for the control method discussed in this study. Additionally, there is a requirement for the system to include instructions that ensure the controlled CAVs depart at the designated time specified by the management. The suggested method of the work is limited by the current level of CAVs, and its effectiveness can only be verified through simulation. Once the technology of CAVs has advanced to a suitable stage in the future, the method described in this paper needs to be evaluated in actual road networks to observe whether it has the potential to be widely used.

Author Contributions: M.S. and L.S. conceived and designed the methodology and model; Y.Z. analyzed the data; Y.Z. interpreted the findings and wrote the paper; and M.S. and L.S. provided revision suggestions. All authors have read and agreed to the published version of the manuscript.

Funding: This research was funded by the National Key Research and Development Project (2019YFE0112100), National Natural Science Foundation of China (Grant No. 52272312), Science, Technology Innovation Action Plan of Shanghai Science and Technology Commission (21dz1203802),

Science, and Technology Innovation Action Plan of Shanghai Science and Technology Commission (20dz1202702), Hebei Provincial Department of Transportation Technology Project: Research on Key Technologies for Intelligent Guarantee and Service of Unclosed Operation of Jingxiong Expressway in Severe Weather (JX-202001), and the Fundamental Research Funds for the Central Universities (without funding number).

Institutional Review Board Statement: Not applicable.

Informed Consent Statement: Not applicable.

Data Availability Statement: The data presented in this study are available on request from the corresponding author.

Acknowledgments: The authors wish to acknowledge the crucial role of our research team (Key Laboratory of Road and Traffic Engineering of the Ministry of Education) members and all stakeholders involved in the data collection and supporting tasks.

Conflicts of Interest: The authors declare no conflict of interest. They declare that they have no relevant or material financial interests that relate to the research described in this paper.

References

1. *The Most Congested Cities in the World*; Cutex Travel: London, UK, 2023.
2. Pishue, B. 2022 *Global Traffic Scorecard*; Global Transportation Analytics Company; INRIX: Washington, DC, USA, 2023.
3. Systematics, C. *Traffic Congestion and Reliability: Trends and Advanced Strategies for Congestion Mitigation*; U.S. Department of Transportation Federal Highway Administration: Washington, DC, USA, 2020.
4. Department for Transport. *Road Traffic Estimates in Great Britain*; Department for Transport: London, UK, 2022.
5. The U.S. Energy Information Administration (EIA). *Congressional Research Service*; The U.S. Energy Information Administration (EIA): Washington, DC, USA, 2020.
6. Campbell, S.; Leach, D.; Valentine, K.; Coogan, M.; Meyer, M.; Casgar, C. *From Handshake to Compact: Guidance to Foster Collaborative, Multimodal Decision Making*; TCRP-NCHRP Report; Transportation Research Board: Washington, DC, USA, 2005.
7. Angelevska, B.; Atanasova, V.; Andreevski, I. Urban air quality guidance based on measures categorization in road transport. *Civ. Eng. J.* **2021**, *7*, 253–267. [[CrossRef](#)]
8. Fenger, J. Urban air quality. *Atmos. Environ.* **1999**, *33*, 4877–4900. [[CrossRef](#)]
9. Hao, J.; Wang, L. Improving urban air quality in China: Beijing case study. *J. Air Waste Manag. Assoc.* **2005**, *55*, 1298–1305. [[CrossRef](#)] [[PubMed](#)]
10. Ha PY, J.; Chen, S.; Dong, J.; Du, R.; Li, Y.; Labi, S. Leveraging the capabilities of connected and autonomous vehicles and multi-agent reinforcement learning to mitigate highway bottleneck congestion. *arXiv* **2020**, arXiv:2010.05436.
11. Qiangqiang, G.; Li, L.; Xuegang, B.J. Urban traffic signal control with connected and automated vehicles: A survey. *Transp. Res. Part C Emerg. Technol.* **2019**, *101*, 313–334.
12. Sugiyama, Y.; Fukui, M.; Kikuchi, M.; Hasebe, K.; Nakayama, A.; Nishinari, K.; Tadaki, S.-I.; Yukawa, S. Traffic jams without bottlenecks—Experimental evidence for the physical mechanism of the formation of a jam. *New J. Phys.* **2008**, *10*, 033001. [[CrossRef](#)]
13. Vickrey, W. Congestion theory and transport investment. *Am. Econ. Rev.* **1969**, *59*, 251–261.
14. *Highway Statistics*; Federal Highway Administration: Washington, DC, USA, 2011.
15. Wang, F.Y. Parallel control and management for intelligent transportation systems: Concepts, architectures, and applications. *IEEE Trans. Intell. Transp. Syst.* **2010**, *11*, 630–638. [[CrossRef](#)]
16. Hamilton, A.; Waterson, B.; Cherrett, T.; Robinson, A.; Snell, I. The evolution of urban traffic control: Changing policy and technology. *Transp. Plan. Technol.* **2013**, *36*, 24–43. [[CrossRef](#)]
17. Savelsbergh, M.; Van Woensel, T. 50th anniversary invited article—City logistics: Challenges and opportunities. *Transp. Sci.* **2016**, *50*, 579–590. [[CrossRef](#)]
18. Tahir, M.N.; Leviäkangas, P.; Katz, M. Connected vehicles: V2V and V2I road weather and traffic communication using cellular technologies. *Sensors* **2022**, *22*, 1142. [[CrossRef](#)] [[PubMed](#)]
19. Wang, B.; Han, Y.; Wang, S.; Tian, D.; Cai, M.; Liu, M.; Wang, L. A Review of Intelligent Connected Vehicle Cooperative Driving Development. *Mathematics* **2022**, *10*, 3635. [[CrossRef](#)]
20. *Automated Vehicles for Safety*; National Highway Traffic Safety Administration (NHTSA): Washington, DC, USA, 2016.
21. Ahmed, H.U.; Huang, Y.; Lu, P.; Bridgelall, R. Technology developments and impacts of connected and autonomous vehicles: An overview. *Smart Cities* **2022**, *5*, 382–404. [[CrossRef](#)]
22. Guo, Q.; Ban, X.J.; Aziz, H.M.A. Mixed traffic flow of human driven vehicles and automated vehicles on dynamic transportation networks. *Transp. Res. Part C Emerg. Technol.* **2021**, *128*, 103–159. [[CrossRef](#)]
23. Li, C.; Yue, W.; Mao, G.; Xu, Z. Congestion propagation based bottleneck identification in urban road networks. *IEEE Trans. Veh. Technol.* **2020**, *69*, 4827–4841. [[CrossRef](#)]

24. Siri, S.; Pasquale, C.; Sacone, S.; Ferrara, A. Freeway traffic control: A survey. *Automatic* **2021**, *130*, 109655. [\[CrossRef\]](#)
25. Han, X.; Shao, M.; Sun, L.; Yuan, Y. A study on Autonomous Vehicles' Driving Behavior Based on Open Road Test Data. In Proceedings of the 2023 7th International Conference on Transportation Information and Safety (ICTIS), Xi'an, China, 4–6 August 2023; pp. 2256–2264.
26. Luo, X.; Li, X.; Shaon, M.R.R.; Zhang, Y. Multi-lane-merging strategy for connected automated vehicles on freeway ramps. *Transp. B Transp. Dyn.* **2023**, *11*, 127–145. [\[CrossRef\]](#)
27. Yang, L.; Zhan, J.; Shang, W.L.; Fang, S.; Wu, G.; Zhao, X.; Deveci, M. Multi-Lane Coordinated Control Strategy of Connected and Automated Vehicles for On-Ramp Merging Area Based on Cooperative Game. *IEEE Trans. Intell. Transp. Syst.* **2023**, *24*, 13448–13461. [\[CrossRef\]](#)
28. Liu, H.; Zhuang, W.; Yin, G.; Li, Z.; Cao, D. Safety-critical and flexible cooperative on-ramp merging control of connected and automated vehicles in mixed traffic. *IEEE Trans. Intell. Transp. Syst.* **2023**, *24*, 2920–2934. [\[CrossRef\]](#)
29. Abdel-Aty, M.; Dilmore, J.; Dhindsa, A. Evaluation of variable speed limits for real-time freeway safety improvement. *Accid. Anal. Prev.* **2006**, *38*, 335–345. [\[CrossRef\]](#)
30. Dowling, R.; Nevers, B.; Jia, A.; Skabardonis, A.; Krause, C.; Vasudevan, M. Performance benefits of connected vehicles for implementing speed harmonization. *Transp. Res. Procedia* **2016**, *15*, 459–470. [\[CrossRef\]](#)
31. Lee, C.; Hellinga, B.; Saccomanno, F. Evaluation of variable speed limits to improve traffic safety. *Transp. Res. Part C Emerg. Technol.* **2006**, *14*, 213–228. [\[CrossRef\]](#)
32. Strömrgren, P.; Lind, G. Harmonization with variable speed limits on motorways. *Transp. Res. Procedia* **2016**, *15*, 664–675. [\[CrossRef\]](#)
33. Malikopoulos, A.A.; Hong, S.; Park, B.B.; Lee, J.; Ryu, S. Optimal control for speed harmonization of automated vehicles. *IEEE Trans. Intell. Transp. Syst.* **2018**, *20*, 2405–2417. [\[CrossRef\]](#)
34. Elfar, A.; Talebpour, A.; Mahmassani, H.S. Predictive Speed Harmonization Using Machine Learning in Traffic Flow with Connected and Automated Vehicles. *Transp. Res. Rec.* **2023**. [\[CrossRef\]](#)
35. Hegyi, A.; Hoogendoorn, S.P.; Schreuder, M.; Stoelhorst, H.; Viti, F. SPECIALIST: A Dynamic Speed Limit Control Algorithm Based on Shock Wave Theory. In Proceedings of the 11th International IEEE Conference on Intelligent Transportation Systems, Beijing, China, 12–15 October 2008; IEEE: Piscataway, NY, USA, 2008.
36. Lighthill, M.J.; Whitham, G.B. On Kinematic Waves II. A Theory of Traffic Flow on Long Crowded Roads. *Proc. R. Soc. Lond. Ser. A Math. Phys. Sci.* **1955**, *229*, 317–345.
37. Richards, P.I. Shock Waves on the Highway. *Oper. Res.* **1956**, *4*, 42–51. [\[CrossRef\]](#)
38. Hegyi, A.; Hoogendoorn, S.P.; Schreuder, M.; Stoelhorst, H. The Expected Effectivity of the Dynamic Speed Limit Algorithm SPECIALIST—A Field Data Evaluation Method. In Proceedings of the European Control Conference (ECC), Budapest, Hungary, 23–26 August 2009; IEEE: Piscataway, NY, USA, 2009.
39. Chen, D.; Ahn, S. Variable Speed Limit Control for Severe Non-Recurrent Freeway Bottlenecks. *Transp. Res. Part C Emerg. Technol.* **2015**, *51*, 210–230. [\[CrossRef\]](#)
40. Peeta, S.; Ziliaskopoulos, A.K. Foundations of Dynamic Traffic Assignment: The Past, the Present and the Future. *Netw. Spat. Econ.* **2001**, *1*, 233–265. [\[CrossRef\]](#)
41. Ran, B.; Boyce, D. *Modeling Dynamic Transportation Networks: An Intelligent Transportation Systems Oriented Approach*; Springer: New York, NY, USA, 1996.
42. Moradi, H.; Sasaninejad, S.; Wittevrongel, S.; Walraevens, J. The contribution of connected vehicles to network traffic control: A hierarchical approach. *Transp. Res. Part C Emerg. Technol.* **2022**, *139*, 103644. [\[CrossRef\]](#)
43. Guo, Q.; Ban, X.J. A multi-scale control framework for urban traffic control with connected and automated vehicles. *Transp. Res. Part B Methodol.* **2023**, *175*, 102787. [\[CrossRef\]](#)
44. Zeng, Y.C.; Shao, M.H.; Sun, L.J.; Chang, L.U. Traffic prediction and congestion control based on directed graph convolution neural network. *China J. Highw. Transp.* **2021**, *34*, 239–248.
45. Kesting, A.; Treiber, M.; Helbing, D. Enhanced intelligent driver model to access the impact of driving strategies on traffic capacity. *Philos. Trans. R. Soc. A Math. Phys. Eng. Sci.* **2010**, *368*, 4585–4605. [\[CrossRef\]](#)
46. Ulungu, E.L.; Teghem, J. Multi-objective combinatorial optimization problems: A survey. *J. Multi-Criteria Decis. Anal.* **1994**, *3*, 83–104. [\[CrossRef\]](#)
47. Ceylan, H.; Bell, M.G.H. Traffic signal timing optimization based on genetic algorithm approach, including drivers' routing. *Transp. Res. Part B Methodol.* **2004**, *38*, 329–342. [\[CrossRef\]](#)
48. Sofronova, E. Variational Genetic Algorithm and Its Application to Urban Traffic Flow Control. *Int. J. Open Inf. Technol.* **2023**, *11*, 3–13.
49. Chai, W.; Zheng, Y.; Tian, L.; Qin, J.; Zhou, T. GA-KELM: Genetic-algorithm-improved kernel extreme learning machine for traffic flow forecasting. *Mathematics* **2023**, *11*, 3574. [\[CrossRef\]](#)
50. Kaffash, S.; Nguyen, A.T.; Zhu, J. Big data algorithms and applications in intelligent transportation system: A review and bibliometric analysis. *Int. J. Prod. Econ.* **2021**, *231*, 107868. [\[CrossRef\]](#)
51. Gen, M.; Lin, L. Genetic algorithms and their applications. In *Springer Handbook of Engineering Statistics*; Springer: London, UK, 2023.
52. SAE International. *Taxonomy and Definitions for Terms Related to Driving Automation Systems for On-Road Motor Vehicles*; SAE International: Warrendale, PA, USA, 2016.

53. Van Arem, B.; Van Driel, C.J.G.; Visser, R. The impact of cooperative adaptive cruise control on traffic-flow characteristics. *IEEE Trans. Intell. Transp. Syst.* **2006**, *7*, 429–436. [[CrossRef](#)]
54. Shladover, S.E.; Su, D.; Lu, X. Impacts of Cooperative Adaptive Cruise Control on Freeway Traffic Flow. *Transp. Res. Rec. J. Transp. Res. Board* **2012**, *2324*, 63–70. [[CrossRef](#)]
55. Liu, H.; Kan, X.; Shladover, S.E.; Lu, X.-Y.; Ferlis, R.E. Modeling impacts of Cooperative Adaptive Cruise Control on mixed traffic flow in multi-lane freeway facilities. *Transp. Res. Part C Emerg. Technol.* **2018**, *95*, 261–279. [[CrossRef](#)]
56. Milanes, V.; Shladover, S.E.; Spring, J.; Nowakowski, C.; Kawazoe, H.; Nakamura, M. Cooperative Adaptive Cruise Control in Real Traffic Situations. *IEEE Trans. Intell. Transp. Syst.* **2014**, *15*, 296–305. [[CrossRef](#)]
57. Zeng, Y.; Shao, M.; Sun, L. Comprehensive Multi-Layered and Time-Dependent Congestion Control Strategy for Mixed Traffic Flow. In Proceedings of the 2023 7th International Conference on Transportation Information and Safety (ICTIS), Xi'an, China, 4–6 August 2023.
58. Friesz, T.L.; Han, K. The mathematical foundations of dynamic user equilibrium. *Transp. Res. Part B Methodol.* **2019**, *126*, 309–328. [[CrossRef](#)]
59. Huang, H.J.; Lam, W.H.K. Modeling and solving the dynamic user equilibrium route and departure time choice problem in network with queues. *Transp. Res. Part B Methodol.* **2002**, *36*, 253–273. [[CrossRef](#)]

Disclaimer/Publisher's Note: The statements, opinions and data contained in all publications are solely those of the individual author(s) and contributor(s) and not of MDPI and/or the editor(s). MDPI and/or the editor(s) disclaim responsibility for any injury to people or property resulting from any ideas, methods, instructions or products referred to in the content.